MOL 48751   1

Imidazoquinolinone, Imidazopyridine and Isoquinolindione Derivatives as Novel and Potent Inhibitors of the Poly(ADP-ribose) Polymerase (PARP): a Comparison with Standard PARP Inhibitors

Tobias Eltze, Rainer Boer, Thomas Wagner, Steffen Weinbrenner, Michelle C. McDonald, Christoph Thiemermann, Alexander Bürkle, and Thomas Klein

Molecular Toxicology, University of Konstanz, Germany (T.E., A.B.); Preclinical Research, NYCOMED GmbH, Konstanz, Germany (R.B., T.W., S.W., T.K.); and William Harvey Research Institute, London, England (M.C.M., C.T.)

Running title: Novel PARP inhibitors

Address correspondence to: Dr. Thomas Klein, Boehringer-Ingelheim Pharma GmbH, 88397 Biberach an der Riss, Germany, Email: thomasth.klein@web.de, or Prof. Alexander Bürkle, Molecular Toxicology Group, University of Konstanz, 78457 Konstanz, Germany, E-mail: Alexander.Buerkle@uni-konstanz.de

Number of text pages: 28

Number of tables: 1

Number of figures: 10

Number of references: 38

Number of words Abstract: 249

Number of words Introduction: 751

Number of words Discussion: 1737

ABBREVIATIONS: PAR, poly(ADP-ribose); PARP-1, poly(ADP-ribose) polymerase-1; PARP-2, poly(ADP-ribose) polymerase-2; BYK49187, 2-[4-(5-methyl-1H-imidazol-4-yl))-piperidin-1-yl]-4,5-dihydro-imidazo[4,5,1-i,j]quinolin-6-one; BYK236864, 2-(4-pyridin-2-yl-phenyl)-4,5-dihydro-imidazo[4,5,1-i,j]quinolin-6-one; BYK20370, 6-chloro-8-hydroxy-2,3-dimethyl-imidazo-[1,2-α]-pyridine; BYK204165, 4-(1-methyl-1H-pyrrol-2-ylmethylene)-4H-isoquinolin-1,3-dione; DPQ, 3,4-dihydroxy-5-[4-(piperidin1-yl)butoxy]isoquinolin-1(2H)-one; PND, 6-(5H)-phenanthridinone; ISQ, 1,5-dihydroxyisoquinoline; NA, nicotinamide; 3-AB, 3-aminobenzamide; 5-AIQ, 5-aminoisoquinolin-1(2H)-one; PJ34, N-(6-oxo-5,6-dihydro-phenanthridin-2-yl)-N,N-dimethylacetamide; GPI-6150, 1,11b-dihydro-[2H]benzopyrano[4,3,2-de]isoquinolin-3-one; 4-ANI, 4-amino-1,8-naphthalimide; 4-HQN, 4-hydroxyquinazoline; INH$_2$BP, 5-iodo-6-amino-1,2-benzopyrone, AAR, area at risk; IS, infarct size.

ABSTRACT

We have identified three novel structures for inhibitors of the poly(ADP-ribose) polymerase
(PARP), a nuclear enzyme activated by strand breaks in DNA and implicated in DNA
repair, apoptosis, organ dysfunction or necrosis. BYK49187 (2-[4-(5-methyl-1H-imidazol-4-
yl))-piperidin-1-yl]-4,5-dihydro-imidazo[4,5,1-i,j]quinolin-6-one), BYK236864 (2-(4-pyridin-2-
yl-phenyl)-4,5-dihydro-imidazo[4,5,1-i,j]quinolin-6-one), BYK20370 (6-chloro-8-hydroxy-
2,3-dimethyl-imidazo-[1,2-α]-pyridine) and BYK204165 (4-(1-methyl-1H-pyrrol-2-
ylmethylene)-4H-isoquinolin-1,3-dione) inhibited cell-free recombinant human PARP-1 with
pIC_{50} values of 8.36, 7.81, 6.40 and 7.35 (pK_i 7.97, 7.43, 5.90 and 7.05), and murine
PARP-2 with pIC_{50} values of 7.50, 7.55, 5.71 and 5.38, respectively. BYK49187,
BYK236864 and BYK20370 displayed no selectivity for PARP-1/2, whereas BYK204165
displayed 100-fold selectivity for PARP-1. The IC_{50} values for inhibition of poly(ADP-ribose)
synthesis in human lung epithelial A549 and cervical carcinoma C4I cells as well in rat
cardiac myoblast H9c2 cells after PARP activation by H_2O_2 were highly significantly
correlated with those at cell-free PARP-1 (r^2 = 0.89 – 0.96, P < 0.001), but less with those
at PARP-2 (r^2 = 0.78 – 0.84, P < 0.01). The infarct size caused by coronary artery
occlusion and reperfusion in the anesthetised rat was reduced by 22% (P < 0.05) by
treatment with BYK49187 (3 mg/kg i.v. bolus and 3 mg/kg/h i.v. during 2 h reperfusion),
while the weaker PARP-inhibitors, BYK236864 and BYK20370 were not cardioprotective.
In conclusion, the imidazoquinolinone BYK49187 is a potent inhibitor of human PARP-1
activity in cell-free and cellular assays in vitro and reduces myocardial infarct size in vivo.
The isoquinolindione BYK204165 was found to be 100-fold selective for PARP-1. Thus,
both compounds might be novel and valuable tools for investigating PARP-1 mediated
effects.

Introduction

Poly(ADP-ribose) polymerases 1 and 2 (PARP-1, -2) are abundant nuclear enzymes in eukaryotic cells that have been implicated in the cellular response to DNA damage (Schreiber et al., 2006). PARPs catalyse an energy consuming reaction by transferring ADP-ribose moieties from the substrate NAD^+ to nuclear acceptor proteins including PARP itself and to existing ADP-ribose adducts on protein, thus forming chains of poly(ADP-ribose) (PAR), in order to render damaged DNA accessible to the repair system and to maintain cell survival, genomic stability and mammalian longevity (D'Amours et al., 1999). This beneficial, cytoprotective effect of PARP activity is apparent under conditions of low to moderate damage infliction. A more intense activation of PARP in response to abundant genotoxic stimuli activates an apoptotic pathway to eliminate cells with insufficiently repaired DNA, mediated via release of apoptosis-inducing factor (AIF) from mitochondria (Yu et al., 2002). Third, severe DNA damage or consequences of a variety of cardiovascular and inflammatory diseases, such as shock, ischemia, diabetes and neurodegenerative disorders, can cause excessive activation of PARP, which depletes the intracellular pools of NAD^+ and subsequently ATP, ultimately leading to cellular dysfunction and necrosis by rapid energy consumption (Pieper et al., 1999; Virág and Szabó, 2002; Amè et al., 2004). Consequently, depending on the circumstances, pharmacological inhibitors of PARP have the potential to either enhance the cytotoxicity of antitumor treatment, or to provide remarkable protection from tissue damage in various forms of reperfusion organ injury, inflammation and neurotoxicity in animal models (Virág and Szabó, 2002; Beneke et al., 2004; Jagtap and Szabó, 2005; de la Lastra et al., 2007). Although the major isoform, PARP-1, encoded by one of the seventeen currently known members of the human *PARP* gene family, was thought to be responsible for all the DNA damage-dependent PAR synthesis in mammalian cells, a second DNA damage-dependent isoform, PARP-2, was subsequently discovered based on the presence of residual DNA-dependent PARP activity in cells from *parp-1$^{-/-}$* mice (Shieh et al., 1998). Recently, distinct binding modes necessary for discrimination between ligands and each isoenzyme have been discovered, enabling synthesis of PARP-1 selective quinazolinones and PARP-2 selective quinoxalines (Iwashita et al., 2004a; Iwashita et al., 2004b; Ishida et al., 2006).

PARP-1 activation contributes to the tissue injury caused by ischemia and reperfusion in various organs including heart (Eliasson et al., 1997; Thiemermann et al., 1997; Liaudet et al., 2001). A reduction in infarct size and/or improved cardiac contractility after myocardial ischemia in rats has been demonstrated for PARP inhibitors of different chemical structure, *e.g.* 3-aminobenzamide (3-AB), nicotinamide (NA), 4-hydroxyquinazoline (4-HQN), 1,5-

dihydroxyisoquinoline (ISQ), 1,11b-dihydro-[2*H*]benzopyrano[4,3,2-de]isoquinolin-3-one
(GPI-6150), 5-aminoisoquinolin-1(2*H*)-one (5-AIQ), N-(6-oxo-5,6-dihydro-phenanthridin-2-
yl)-N,N-dimethylacetamide (PJ34) and INO-1001, an isoindolinone derivative
(Thiemermann et al., 1997; Zingarelli et al., 1997; Bowes et al., 1998; Docherty et al.,
1999; McDonald et al., 2000; Pieper et al., 2000; Wayman et al., 2001; Faro et al., 2002).
However, their PARP inhibitory effect in vivo is not solely determined by their potency in
vitro, but most notably governed by their ability to cross cell membranes and their low
lipophilicity. Thus, although different new chemical structures of potent PARP inhibitors
have been discovered in the last decade (Southan and Szabó, 2003; Jagtap and Szabó,
2005), the need for developing selective inhibitors that are both potent and sufficiently
water-soluble is still of pivotal importance (Woon and Threadgill, 2005).

In the present study, we describe the biochemical and pharmacological properties of two
new imidazoquinolinone compounds, BYK49187 and BYK236864, the imidazopyridine
BYK20370, as well as the isoquinolindione BYK204165, of which only the latter compound
bears a benzamide structure mimicking to some degree the nicotinamide moiety of the
substrate NAD$^+$ (Fig. 1). We characterized these compounds with respect to inhibitory
potency and selectivity on cell-free recombinant human PARP-1 and murine PARP-2,
including analysis of their kinetics and reversibility of PARP-1 inhibition. We also tested the
compounds in various cellular systems, i.e. human lung epithelial A549, human cervical
carcinoma C4I, and rat cardiac myoblast H9c2 cells, in comparison with a series of
standard PARP inhibitors of various chemical classes and potencies. Two of the new
compounds were tested for inhibition of PARP in *parp-1*$^{+/+}$ and *parp-1*$^{-/-}$ mouse fibroblasts.
Additionally, we evaluated three of the compounds for their ability to reduce myocardial
reperfusion injury measured as infarct size in the anesthetised rat, a reliable model in
which treatment with PARP-inhibitors of different chemical structures have been shown to
reduce the infarct size and to improve cardiac contractility (Bowes et al., 1998; Docherty et
al., 1999; Pieper et al., 2000; Wayman et al., 2001; Virág and Szabó, 2002; Szabó et al.,
2004).

Methods

PARP-1 assay

The enzymatic reaction of the recombinant human PARP-1 was performed by scintillation proximity assay (SPA) run in a 384-well format using microtiter F-plates (781095; Greiner, Frickenhausen, Germany). The assay was carried out in a total volume of 50 µl comprising 100 mM Tris-HCl (pH 7.8), 10 mM MgCl$_2$, 10 mM dithiothreitol, 1 µM nicotinamide adenine dinucleotide (NAD$^+$), 0.067 µCi of [^{3}H]NAD$^+$ (Amersham, UK), 1 µg double-stranded oligonucleotides GGAATTCC (ARK Scientific, Darmstadt, Germany), 100 ng PAR antibody (Dr. M. Frey; Steinbeis-Transfer Centre, Mannheim, Germany, or Alexis Corp., 10H-P5-0799), in the absence and presence of various concentrations of PARP inhibitors (dissolved in DMSO). Final DMSO concentrations in the assay did not exceed 0.3%. An equal amount of vehicle was added to the control samples. The enzymatic reaction was started by adding 75 ng of recombinant partially purified human PARP-1 (Dr. M. Frey; Steinbeis-Transfer Centre, Mannheim, Germany). After vigorous shaking of the microtiter-plates for a few minutes, protein-A coated SPA-PVT beads (RPN Q0019; Amersham, UK) were added. The mixture was vortexed again and kept at room-temperature for 18 to 20 h. Bead-bound radioactivity (counts per minute) was measured by liquid scintillation spectrometry.

NAD$^+$ concentrations were 1 µM to calculate the pIC$_{50}$ values for all compounds for half-maximal inhibition of enzyme activity, and varied from 0.2 to 200 µM for determination of K_m value of the substrate and for analyzing the type of inhibition of the novel compounds by Lineweaver-Burk plots as well as for determination of pK_i values by Schild plots. In the latter case, three to four different inhibitor concentrations spaced by a factor of 2.5 to 3 (0.4 to 0.5 log units) were used for graphical calculation of pK_i and slope of regression. All experiments were performed in duplicate or more, and the average of the results was used for analysis.

PARP-2 assay

Similarly, the enzymatic reaction of the recombinant mouse PARP-2 was quantified by scintillation proximity assay (SPA) run on a 96-well format using microtiter V-plates (1450-514, Wallac Isoplate TM). At the time these experiments were initiated human PARP-2 was not available. When it became available during the course of the experiments, we decided to continue with the murine enzyme for consistency. The assay was carried out in a total volume of 100 µl comprising 100 mM Tris-HCl (pH 7.8), 10 mM MgCl$_2$, 10 mM dithiothreitol, 1 µM NAD$^+$, 0.067 µCi of [^{3}H]NAD$^+$, 100 ng PAR antibody (10H-P5-0799;

Alexis Corp.), 100 ng recombinant mouse PARP-2 (Alexis Corp.) initially dissolved in 50 mM Tris-HCl (pH 7.5), 14 mM β-mercaptoethanol, 0.5 mM PMSF (phenylmethylsulfonylfluoride) and 10% glycerol, protein A coated SPA-PNT antibody-binding beads (RPN Q0019; Amersham, UK), in the absence or presence of various concentrations of PARP inhibitors (dissolved in DMSO). Final DMSO concentrations in the assay did not exceed 0.3%. An equal amount of the vehicle was added to the control samples. The enzymatic reaction was started by adding 1 μg double-stranded calf thymus DNA (DNAse digested, Sigma) and incubated at room temperature during shaking for 60 min and was then incubated for 16 h overnight. Radioactivity incorporated from [^{3}H]NAD$^+$ into PAR, and then being captured by PAR antibody and finally bound to SPA beads was measured by liquid scintillation spectrometry.

Immunofluorescence analysis of PAR in fibroblasts

Mouse embryonic fibroblasts (3T3) from *parp-1*$^{+/+}$ and *parp-1*$^{-/-}$ mice were cultured to confluence in Dulbecco´s modified Eagle´s medium containing 4.5 g/l glucose supplemented with 0.58 g/l L-glutamine, penicillin G (100 units/ml), streptomycin (100 μg/ml) and 10% heat-inactivated fetal calf serum (FCS) at 37°C in a humidified 5% CO_2-95% air incubator. Confluent cells were washed in PBS and treated as described below. For immunofluorescence analysis of PAR, cells were trypsinized, plated on sterile coverslips at a density of $2x10^4$ cells/cm^2 in 12-well culture dishes and allowed to adhere overnight (Wagner et al., 2007). Following exposure of cultures to the inhibitor (0.3 – 3 μM or 0.3 - 10 μM, final DMSO concentration 0.3%) for 30 min, cells were washed with PBS and treated with H_2O_2 (5 mM for *parp-1*$^{+/+}$ fibroblasts, 50 mM for *parp-1*$^{-/-}$ fibroblasts) for 5 min at 37°C to stimulate PAR formation. Cells were then fixed (methanol/acetic acid, 3:1 [v/v]) for 10 min at room temperature. After three washings with PBS, cells were incubated with monoclonal antibody 10H directed against PAR at a dilution of 1:250 in blocking solution (5% milk powder in PBS, 0.05% Tween 20) for 1 h at 37°C in a humid chamber. After three washings with PBS, antibody-antigen complexes were detected with Alexa-488-conjugated goat secondary antibody (Sigma, Deisenhofen, Germany) for 45 min at 37°C. The cells were washed three times and then counterstained with 4´,6´-diamidino-2-phenylindole (DAPI). Cells were examined under a fluorescence microscope for detection of PAR.

Cellular PARP assay

Human cervical carcinoma C4I cells (ATCC, CRL-1594), human lung epithelial A549 cells and rat cardiomyocytes H9c2 (ATCC, CRL-1446) were grown to confluence in culture flasks containing minimum essential medium (RPMI-1640, Sigma) and 10% FCS. After

reaching confluence, cells were trypsinized (0.05%). After centrifugation at 50xg for 5 min, pelleted cells were resuspended in RPMI-1640 medium containing 2 mM L-glutamine. Cells were incubated in 96-wells for 3 days at 37°C until confluency was reached. At this time point the cell number was between 2-5x10^4 cells/96-well. Cellular supernatant was removed from the wells by aspiration and wells were washed once with 100 µl DMEM. 60 µl of DMEM was added onto the adherent cell layer. Inhibitor dilution series were prepared in 100% DMSO and diluted 100-fold in DMEM. Thirty µl of inhibitor solution was addded to 60 µl of DMEM in each well yielding a total of 90 µl inhibitor/DMEM solution, with a final DMSO concentration of 0.3%. Cells were preincubated with inhibitors for 30 min, then intracellular PARP was activated by the addition of 10 µl H_2O_2 (10 mM; final concentration 1 mM). Cells were incubated for 10 min at 37°C. The reaction was terminated by adding 100 µl fixation solution (70% methanol /30% acetone [v/v]; precooled to -20°C) for 10 min. The supernatant was aspirated and plates were dried for 30 min. For re-hydration of the cells 100 µl of phosphate buffer saline (PBS) was added for 10 min at room temperature. PBS was removed by aspiration and 100 µl of blocking solution (5% milk powder in PBS containing 0.05% Tween 20) was added to each well followed by 30 min incubation at room temperature. After removal of the blocking solution mouse monoclonal PAR-antibody 10H (final concentration 20 µg/ml, Steinbeis-Transfer Centre, Mannheim) was added in 100 µl of blocking solution. Cells were incubated for 1 h at 37°C. Wells were washed twice for 5 min with 100 µl Tween 20/PBS and the secondary FITC-conjugated goat anti mouse antibody (F-4018, 50-fold dilution in blocking buffer; Sigma) was added. Cells were incubated for 30 min at 37°C and then washed two times with 100 µl Tween 20/PBS. Fluorescence was measured with the dry plates in a fluorescence counter (Victor; Wallac) at 485/536 nm.

All compounds were subjected to a uniform solution and dilution procedure, with DMSO as solvent not exceeding final concentrations of 0.3% in all non-cellular and cellular assays. In accordance with previous observations (Banasik et al., 2004), this DMSO concentration did not interference with the cell-free and cellular assay systems.

Coronary artery ligation and myocardial infarct size in the rat
The method of coronary artery occlusion and reperfusion in the anesthetised rat was performed as previously described (Wayman et al., 2001). The care and the use of animals in this work were in accordance with UK Home Office guidelines on the Animals (Scientific Procedures) Act 1986 and the European Community guidelines for the use of experimental animals. Wistar rats (male, 200-300 g; Tuck, Rayleigh, Essex, UK) receiving standard diet and water *ad libitum*, were anesthetised with thiopentone sodium (Intraval[®],

120 mg/kg i.p.; Rhône-Merrieux, Essex, UK) and thereafter intubated and ventilated with a Harvard ventilator. Body temperature was maintained at 38 ± 1ºC. The right carotid artery was cannulated and connected to a pressure transducer (MLT 1050; AD Instruments Ltd, Hastings, UK) to monitor mean arterial blood pressure (MAP) and heart rate (HR). The right jugular vein was cannulated for administration of drugs and Evans Blue (at the end of the experiment). A lateral thoracotomy was performed and the heart was suspended in a temporary pericardial cradle. A snare occluder was placed around the left anterior descending coronary artery (LAD), after that the animals were allowed to stabilise for 30 min prior to LAD ligation. The coronary artery was occluded at time 0, and at 20 min into myocardial ischemia, a bolus injection of either vehicle or test compound was administered i.v. After 25 min of acute myocardial ischemia, the occluder was re-opened to allow the reperfusion for 2 h, during which the vehicle or test compound was continuously infused, after that the coronary artery was re-occluded and Evans Blue (1 ml of 2% w/v) injected into the left ventricle, via the right jugular vein cannula, to distinguish between still perfused and non-perfused (area at risk, AAR) sections of the heart. After death of the animals by an overdose of anesthetic, the heart was excised and sectioned into slices of 3-4 mm. The right ventricular wall was removed, and the AAR (pink) was separated from the non-ischemic (blue) area for determination of AAR portion in percent of the left ventricular portion. The AAR was cut into small pieces and incubated with p-nitroblue tetrazolium (NBT, 0.5 mg/ml) for 30 min at 37°C. In the presence of intact dehydrogenase enzyme systems in viable myocardium, NBT forms a dark blue formazan, whilst areas of necrosis lack dehydrogenase activity and therefore fail to stain. Pieces were separated according to staining and weighed to determine the infarct size (IS) as a percentage of the weight of the AAR.

The following groups of animals (all n = 10) were studied: (1) Sham-operated control group of rats subjected to the surgical procedure alone (without LAD occlusion) and treated with vehicle (20% polyethylene glycol-400 [PEG, Serva], 15% 1N HCl, 65% distilled water); (2) Vehicle control group of rats subjected to myocardial ischemia for 25 min followed by reperfusion (2 h) and treated with vehicle; (3) Treatment groups of rats subjected to myocardial ischemia and reperfusion and treated with BYK49187, BYK236864 or BYK20370 at 1 or 3 mg/kg i.v. (each n = 10). BYK204165 was not investigated in vivo, due to its poorer water-solubility and its short half-time of 23 min measured at rat microsomes in vitro, compared with the other compounds with $t_{1/2}$ values > 40 min (not shown).

The test compounds were initially dissolved in polyethylene glycol-400 (PEG, Serva) and then diluted to the necessary concentrations with 1N HCl and distilled water. The final concentrations of PEG and 1N HCl were 20% and 15% (v/v), respectively.

Ex vivo PARP-1 assay

At the end of experiment, venous blood samples were taken (in EDTA coated tubes) under anesthesia. Blood plasma was generated via centrifugation ($2250 \times g$, 10 min, 4°C) and stored at -80°C. The ex vivo PARP-1 assay was done in analogy as described but respective blood samples were added instead of test drug solutions.

Lactate dehydrogenase assay (LDH assay)

Cellular toxicity was determined by LDH release measured by the CytoTox 96 assay kit from Promega (Mannheim, Germany).

Materials

BYK49187 (2-[4-(5-methyl-1*H*-imidazol-4-yl))-piperidin-1-yl]-4,5-dihydro-imidazo[4,5,1-i,j]quinolin-6-one), BYK236864 (2-(4-pyridin-2-yl-phenyl)-4,5-dihydro-imidazo[4,5,1-i,j]quinolin-6-one), BYK20370 (6-chloro-8-hydroxy-2,3-dimethyl-imidazo-[1,2-α]-pyridine), and BYK204165 (4-(1-methyl-1*H*-pyrrol-2-ylmethylene)-4*H*-isoquinolin-1,3-dione) were synthetized at NYCOMED AG (formerly ALTANA Chemical Research, Konstanz, Germany). 1,5-Dihydroxyisoquinoline (ISQ), 4-amino-1,8-naphthalimide (4-ANI), nicotinamide (NA), 3-aminobenzamide (3-AB), 3,4-dihydro-5-[4-(piperidinyl1-yl)butoxy]isoquinolin-1(2*H*)-one (DPQ), 4-hydroxyquinazoline (4-HQN), 6-(5*H*)-phenantridinone (PND), 5-iodo-6-amino-1,2-benzopyrone (INH$_2$BP), 5-aminoisoquinolin-1(2*H*)-one (5-AIQ), 1,11b-dihydro-[2*H*]benzopyrano[4,3,2-de]isoquinolin-3-one (GPI-6150), and N-(6-oxo-5,6-dihydro-phenanthridin-2-yl)-N,N-dimethylacetamide (PJ34) were purchased from Alexis Corp. (Läufelfingen, Switzerland).

Human recombinant PARP-1 was supplied by Dr. M Frey (Steinbeis-Transfer Centre, Mannheim, Germany). Mouse recombinant PARP-2 was obtained from Alexis Corp. (Läufelfingen, Switzerland). [^{3}H]NAD$^+$ was purchased from Amersham (now Perkin Elmer, UK). Monoclonal antibody against PAR was from Alexis Corp. (10 µg/ml, 10H-P5-0799) or from Dr. M. Frey (Steinbeis-Transfer Centre, Mannheim, Germany). Goat anti-mouse antibody (85 µg/ml, FITC) was from Sigma, Deisenhofen, Germany. All other chemicals were from commercial suppliers with highest grade of purity.

Statistical analysis

The pIC_{50} values of test compounds for half-maximal inhibition of cell-free PARP-1 and PARP-2 as well of PARP in the cell lines were calculated from concentration-response curves by using Prism 5.0 (GraphPad Inc., San Diego, CA). In analogy to antagonist-receptor interaction, Schild plots were constructed from data derived from enzyme kinetic experiments to estimate the pK_i value of the inhibitor and the slope of regression as an important parameter in that it defines whether or not the data fit the simple competitive model of substrate-inhibitor interaction. Calculation of the correlation coefficient r^2 and the slope of regression line of data using two sets of inhibitory potencies (pIC_{50} values) were performed to compare the results obtained from different experimental assays. All data are presented as means $\pm$ S.E.M. Infarct size in rats was analyzed by 1-factorial ANOVA, followed by a Dunnett's test for comparison of a treated group to the vehicle or sham group. P values < 0.05 are considered statistically significant.

Results

Structure and solubility of BYK49187, BYK236864, BYK20370 and BYK204165

Figure 1 shows the imidazoquinolinones BYK49187 and BYK236864, the imidazopyridine BYK20370, as well as the isoquinolindione BYK204165, of which only the latter compound bears the benzamide moiety, typically present in known PARP inhibitors like 3-AB, PND, GPI-6150, DPQ or 4-ANI. With the exception of 3-AB, NA, 4-ANI, 5-AIQ and INH$_2$BP, which are known to be readily soluble in saline, all reference compounds, including PND, DPQ, GPI-6150 and ISQ, were relatively insoluble in water, which was also true for BYK49187, BYK236864, BYK20370 and BYK204165 with maximal attainable concentrations in saline of 0.42, 0.02, 2.0 and 0.009 mM, mirrored by calculated logP values of 2.3, 3.8, 2.5 and 2.3, respectively (Table 1). Therefore, regardless of their solubility all test compounds were dissolved in DMSO and further diluted in 10% DMSO to the desired test drug concentrations. Final DMSO concentrations in cell-free and cellular PARP-inhibition assays did not exceed 0.3%, a concentration known to exert no inhibitory effect on PARP-1 activity (Banasik et al., 2004).

Identification of compounds of the imidazochinolinone, imidazopyridine and isoquinolindione structure as potent inhibitors of human PARP-1

In our cell-free recombinant human PARP-1 assay, enzymatic activity was measured by quantification of pmol [^{3}H]ADP-ribose bound to antibody binding beads within 24 h by using a low substrate concentration of 1 µM NAD$^+$. This rapid and reliable biochemical screen, using parts of the compound library at NYCOMED AG (formerly ALTANA Pharma AG, Konstanz), identified two imidazochinolinones, BYK49187 and BYK236864, and the isoquinolindione BYK204165 as potent inhibitors of human PARP-1, whereas the imidazopyridine BYK20370 was less potent. Mean pIC$_{50}$ values were 8.36, 7.81, 7.35 and 6.40 for BYK49187, BYK236864, BYK204165 and BYK20370, respectively. The slope values of the inhibition curves were near unity pointing to a homogeneous population of enzyme and an NAD$^+$ competitive behaviour of all compounds (Table 1). None of the reference compounds, e.g. PJ34, 4-ANI, GPI-6150 and PND with pIC$_{50}$ values of 7.72, 7.66, 7.08 and 7.07, reached the nearly nanomolar potency of BYK49187 for inhibition of PARP-1, but were 5- to 20-fold weaker. Among the other compounds investigated, 3-AB and NA proved to be the weakest inhibitors of PARP-1 (pIC$_{50}$ 4.89 and 4.30, respectively) (Table 1).

The selectivity of the compounds was then assessed by inhibition of recombinant mouse PARP-2, using the same low substrate concentration (1 µM NAD$^+$) as in the PARP-1

assay. Potencies for inhibition of PARP-2 (pIC_{50} values) by BYK49187 (7.70), BYK236864 (7.55), BYK20370 (5.71) and all reference inhibitors investigated were less than 0.7 log units (*i.e.* factor of 5) lower than those for inhibition of PARP-1, and by definition these compounds must be regarded as unselective, although some compounds, *e.g.* PND, DPQ and 4-HQN, together with BYK49187 and BYK20370, discriminated both isoforms by a factor of >3 but <5, thereby displaying a small preference for PARP-1 (Table 1). By contrast, the isoquinolindione BYK204165 discriminated between PARP-1 and PARP-2 by a factor of 100 (pIC_{50} 7.35 versus 5.38).

NAD^+ competitive inhibition and reversibility of human PARP-1 by BYK49187, BYK236864, BYK20370 and BYK204165

The mechanism of inhibition of human PARP-1 was investigated by measurement of enzyme velocity at increasing NAD^+ concentrations (0.2 up to 200 μM) in the absence and presence of increasing inhibitor concentrations. In the absence of inhibitor, K_m values were between 5 and 9 μM and V_{max} values between 7 and 11 pmol [^{3}H]ADP-ribose/mg bead bound enzyme. Addition of BYK49187 (10 - 300 nM), BYK236864 (50 - 400 nM), BYK20370 (1 - 30 μM) or BYK204165 (30 nM - 3 μM) resulted in rightward shifts of the apparent K_m value of NAD^+, whereas V_{max} of the reaction essentially did not change (Figs. 2 - 5). The Lineweaver-Burk plots shown in these figures demonstrate that all compounds acted as NAD^+ competitive inhibitors. By analyzing the data in respective Schild plots for determination of inhibitor pK_i values from the intercepts with the abscissa, the following values were obtained: BYK49187 pK_i 7.97 (slope = 0.64; significantly different from unity, $P < 0.01$), BYK236864 pK_i 7.43 (slope = 1.06; not significantly different from unity, $P > 0.05$), BYK20370 pK_i 5.90 (slope = 0.94; not significantly different from unity, $p > 0.05$) and BYK204165 pK_i 7.05 (slope = 0.98; not significantly different from unity, $P > 0.05$). Generally, affinity constants (pK_i values) were in good agreement with respective pIC_{50} values, but on average 0.4 log units lower, which can be explained by the fact that the latter were determined at a lower NAD^+ concentration (1 μM) than its K_m value (> 5 μM).

Consistent with the Lineweaver-Burk plots, data from dilution experiments confirmed that even total inhibition of PARP-1 by BYK49187, BYK236864, BYK20370 and BYK204165 (at starting concentrations 100-fold of the respective IC_{50} values) was fully reversible after a 1,000-fold dilution in assay buffer with constant substrate concentration (1 μM NAD^+), thereby reaching an enzyme activity comparable to that in the absence of inhibitors (100%). In each case, a half-maximal reversal of PARP-1 inhibition approximately occurred by a 100-fold dilution of each starting concentration, enabling calculation of pIC_{50} values that did not differ by more than 0.2 log units from those previously determined by single concentrations (not shown).

Inhibition of PAR formation in *parp-1^{+/+}* and *parp-1^{-/-}* mouse fibroblasts

To confirm PARP-1 selectivity of BYK204165, we further investigated this compound in comparison with the unselective BYK236864 in *parp-1^{+/+}* and *parp-1^{-/-}* fibroblasts. Nuclear PAR was visualised by immunofluorescence analysis using the PAR-specific monoclonal antibody 10H. The assay demonstrated the characteristic granular distribution pattern of PAR formation in nuclei upon DNA-damaging treatment of the cells with H_2O_2 (Fig. 6). The unselective inhibitor BYK236864 completely abrogated immunostaining at 3 µM and above in both cell lines, whereas the PARP-1 selective inhibitor BYK204165 did not preclude residual PAR formation, even at 10 µM in *parp-1^{+/+}* or at 3 µM in *parp-1^{-/-}* fibroblasts. The latter finding is perfectly compatible with ongoing PARP-2 activity in both cell lines and clearly demonstrates the high selectivity of BYK204165 for PARP-1.

Inhibition of PARP in various intact cells

The cellular potency of PARP inhibition by the compounds and standard inhibitors was tested in human lung epithelial A549, human cervical carcinoma C4I and rat cardiomyocyte H9c2 cells, in which activation of PARP was performed by addition of H_2O_2. None of the compounds (BYK49187, BYK236864, BYK20370 and BYK204165) showed cellular toxicity up to 100 µM as evidenced by the lack of detectable LDH activity in cellular supernatants.

PAR formation in A549, C4I and H9c2 cells was inhibited by BYK49187 with pIC_{50} values of 7.80, 7.02 and 7.65, respectively (Table 1). However, the other imidazoquinolinone, BYK236864, which has been shown to be only 3-fold weaker than BYK49187 at cell-free human PARP-1, was 10- to 25-fold weaker than BYK49187 in these cellular assays (pIC_{50} 6.41 in A549 cells and 6.70 in H9c2 cells), possibly due to its lower membrane permeability (20-fold) as compared to BYK49187. The cellular potencies of the less water-insoluble imidazopyridine BYK20370 (pIC_{50} 6.02 - 6.51) were comparable to the value derived from the cell-free PARP-1 assay (pIC_{50} 6.40), whereas those of the less water-soluble isoquinolindione BYK204165 differed from the cell-free assay value by more than 5-fold (Table 1). From the reference compounds investigated in these cellular assays, once again 4-ANI was the most potent inhibitor but did not reach the potency of BYK49187. The respective pIC_{50} values for 4-ANI in A549, C4I and H9c2 cells were 6.88, 6.24 and 6.94, whereas 3-AB together with 4-HQN, INH_2BP and NA was one of the weakest inhibitors (Table 1). Concentration-response curves of BYK49187, BYK236864, BYK20370 and BYK204165 for inhibition of PARP in A549 and H9c2 cells are depicted in Fig. 7.

Although the correlation of pIC_{50} values of the compounds derived from PARP inhibition in A549 cells with those obtained in C4I cells were highly significant (r^2 = 0.97, P < 0.001; slope = 0.97 ± 0.07, mean ± S.E.M., n = 12), generally 3- to 10-fold higher concentrations were necessary to achieve half-maximal inhibition of PARP in C4I cells, possibly reflecting a higher endogenous NAD^+ concentration in these cells (Fig. 8A). An even better correlation (r^2 = 0.97, P < 0.001; slope = 1.05 ± 0.06, mean ± S.E.M., n = 13) was obtained by comparing the pIC_{50} values of the compounds in A549 cells with respective values in rat cardiac myoblast H9c2 cells, strongly suggesting comparable penetration of the compounds into these cells, despite uncertainty about their intracellular NAD^+ substrate concentrations (Fig. 8B).

As a further analysis, we compared the pIC_{50} values obtained from cell free human PARP-1 and mouse PARP-2 assays with respective values of the compounds derived from the three cell lines (Fig. 9). Generally, the IC_{50} values for inhibition of PAR synthesis in A549, C4I and H9c2 cells after PARP activation by H_2O_2 were 3- to 35-fold higher than at the cell-free human PARP-1. Increasingly better correlations and slopes closer to unity were obtained by comparing PARP-1 values with those at A549 cells (r^2 = 0.89, P < 0.001; slope = 0.78 ± 0.08, mean ± S.E.M., n = 13), at C4I cells (r^2 = 0.92, P < 0.001; slope = 0.83 ± 0.08, mean ± S.E.M., n = 12) and finally at H9c2 cells (r^2 = 0.96, P < 0.001; slope = 0.87 ± 0.06, mean ± S.E.M., n = 13). Except for BYK236864, there was no great difference in loss of potency in cellular PARP assays related to cell-free PARP-1 assay between known inhibitors with good water-solubility, *e.g.* 3-AB, 4-ANI, PJ34, INH_2BP and 5-AIQ, and those with poor water-solubility, *e.g.* DPQ, PND, ISQ and GPI-6150, suggesting that different penetration rates of the compounds into the cells were probably not responsible for this effect, but should be related to higher endogenous NAD^+ concentrations within the cells. Less significant correlations were obtained by comparing pIC_{50} values derived from mouse PARP-2 assay with those at A549 cells (r^2 = 0.78, P < 0.01; slope = 0.71 ± 0.06, mean ± S.E.M., n = 13), C4I cells (r^2 = 0.84, P < 0.01; slope = 0.79 ± 0.09, mean ± S.E.M., n = 12) and H9c2 cells (r^2 = 0.83, P < 0.01; slope = 0.79 ± 0.09, mean ± S.E.M., n = 13), thereby excluding a major participation of PARP-2 activation in these cells in response to H_2O_2 treatment. Interestingly, the correlations comparing pIC_{50} values of the inhibitors between the cell-free PARP-1, PARP-2 and cellular PARP assay(s) generated slopes of regression lines consistently being less than unity, which may lead to an apparent underestimation of the more potent drugs in the cellular assays. However, this might be readily explained by a lower drug diffusion gradient and, consequently, a longer time to reach equilibrium

between aqueous medium and intracellular space due to lower concentrations needed for those more potent drugs to calculate their IC_{50} values.

Effect of test drugs on myocardial infarct size in the rat

In the rat model for regional myocardial infarction, mean values for the area at risk (AAR) were similar in all groups studied and ranged from 42 to 52% irrespective of treatment with vehicle (PEG plus HCl) or test drugs (Fig. 10A). In animals treated with vehicle, occlusion of the LAD (for 25 min) followed by reperfusion (for 2 h) resulted in an infarct size of $57 \pm 3\%$ of the AAR (mean $\pm$ S.E.M., n = 11). Intravenous administration of the lower dose of BYK49187 (1 mg/kg bolus followed by 1 mg/kg/h infusion) was nearly ineffective (6% reduction in infarct size; not significantly different from vehicle, $P > 0.05$), whereas the higher dose (3 mg/kg followed by 3 mg/kg/h) caused a significant reduction in infarct size of 22% when compared to vehicle ($P < 0.05$; Fig. 10B). Sham operation alone did not result in a significant degree of infarction in any of the animal groups studied (< 2% of the AAR). The other test drugs investigated in this model, which had an approximately 5- to 100-fold lower potency to inhibit PARP-1 in cell-free and cellular test system(s), *i.e.* BYK236864 and BYK20370 (1 mg/kg i.v. followed by 1 mg/kg/h i.v., and 3 mg/kg i.v. followed by 3 mg/kg/h i.v.), neither reduced nor increased myocardial infarct size (not shown). BYK204165, due to its poorer water-solubility was not tested in vivo.

In order to gain insight into the pharmacokinetic properties of the compounds tested in vivo, blood samples from drug-treated rats were drawn at the end of each drug infusion and tested for their ability to inhibit human PARP-1. Blood samples of rats treated with 3 mg/kg i.v. BYK236864 or BYK49187 significantly inhibited PARP-1 by 54% and 80%, respectively, compared to sham operation (both $P < 0.001$), whereas no significant inhibition (13%, $P > 0.05$) was observed with the same dose of BYK20370 (Fig. 10C).

Discussion

In search for various chemical compounds as potential inhibitors for PARP-1, we found three new chemical entities that comprised imidazoquinolinone, imidazopyridine or isoquinolindione structure. Both imidazoquinolinones, *i.e.* BYK49187 and BYK236869, as well as the imidazopyridine, BYK20370, lack the classical benzamide structure as a mimic of the nicotinamide moiety of the substrate NAD^+, whereas the isoquinolindione BYK204165 formally resembles substituted naphthalimides containing the constrained arylamide motif, which has become one of the consensus pharmacophore for drug design of PARP-1 inhibitors, and of which 4-amino-1,8-naphthalimide (4-ANI) represents its best known member (Schlicker et al., 1999).

Using recombinant human PARP-1 and murine PARP-2 as target enzymes, we investigated all compounds under the same experimental conditions. Since most of the reported compounds are NAD^+ competitive and the respective pIC_{50} values are therefore directly dependent on the substrate concentration used in the assay system, all compounds were tested at a NAD^+ concentration (1 µM) lower than K_m (5 - 9 µM), in order to get reliable estimates of their inhibitory potency and to avoid errors inherent to the use of higher substrate concentrations. Under these conditions, pIC_{50} values determined from concentration-response curves approach the respective pK_i values (Cheng and Prusoff, 1973). We also calculated IC_{50} in the presence of 50 µM NAD^+ for our lead compounds. The IC_{50} values for BYK49187, BYK236864, BYK20370 and BYK204165 increased by a factor of 19, 65, 25 and 45, respectively, reflecting quite well the higher substrate concentration in the cellular assays (see below).

Of all inhibitors investigated in this study, BYK49187 and BYK236864 were the most potent drugs with IC_{50} values both on PARP-1 and PARP-2 approaching the nM range, followed by 4-ANI and PJ34. A second group of compounds with inhibitory activity in the 100 nM range comprised GPI-6150, PND and ISQ. Medium affinity in the µM range for both isoenzymes were found for DPQ, BYK20370 and 5-AIQ, while INH_2BP, 4-HQN and 3-AB had IC_{50} values in the 10 µM range. Interestingly, BYK204165 was more potent at PARP-1 (pIC_{50} 7.35) than at PARP-2 (pIC_{50} 5.38), thus being 100–fold selective for PARP-1, whereas all other drugs investigated did not reach a factor of 10, and in this respect must be classified unselective. The ability of PND to weakly discriminate between PARP-1 and PARP-2 by a factor of 3 has been previously reported (Perkins et al., 2001) and was confirmed in the present study, whereas PJ34 and 3-AB have been characterized as unselective inhibitors (Iwashita et al., 2004b). In accordance with previous data (Zhang et al., 2000), there was no selectivity for GPI-6150 between PARP isoenzymes.

In kinetic experiments with human PARP-1, BYK49187, BYK236864 and BYK204165 exhibited potent and competitive inhibition of enzyme activity, yielding pK_i values of 7.97, 7.43 and 7.05, respectively, whereas BYK20370 was found to be less potent (pK_i 5.90). Consistent with the kinetic analysis demonstrating a competitive type of inhibition of PARP-1 by BYK49187, BYK236864, BYK20370 and BYK204165, dilution experiments revealed that even total inhibition of PARP-1 by high concentrations of all compounds is fully reversible after dilution in assay buffer. Relating to potency on PARP-1, BYK49187 was identified as a PARP-1 inhibitor in the near nanomolar range and is comparable to recently described potent inhibitors, such as AG14361 (pK_i 8.3; Calabrese et al., 2004) and KU0058684 (pIC_{50} 8.4; McCabe et al., 2005).

Inhibition of cellular PAR synthesis in response to H_2O_2 treatment by BYK49187, BYK20370 and BY204165 in human A549 and C4I cells as well in rat H9c2 cells after PARP activation, showed only 2- to 5-fold lower pIC_{50} values than at the isolated human PARP-1 enzyme. BYK236864, probably due to its poorer water-solubility and higher lipophilicity, lost potency by a factor about 10 in all cellular assays. This is line with the observation that 3-AB together with NA, having the lowest logP values, displayed the smallest loss in potency in cellular assays. By and large, the potencies of inhibitors at the isolated human PARP-1 satisfactorily reflect potency at the cellular level and were correlated with high significance ($P < 0.001$), particularly in H9c2 cells. With regard to potency, there is a good compatibility of data between the cell-free and these three cellular assay systems, however, a complete congruence cannot be expected as the cellular uptake of different structural classes of compounds varies due to their different physicochemical properties (*e.g.* logP values). Interestingly, increasingly better correlations were obtained by comparing potencies of the inhibitors from the cell-free human PARP-1 assay with respective values derived from the three cell lines, i.e. A549 cells < C4I cells < H9c2 cells, which renders the latter cell system an attractive and reliable model particularly suitable for assessment of human PARP-1 inhibition at the cellular level. Less significant correlations were obtained by comparing pIC_{50} values of the inhibitors at the three cell lines with respective values from mouse PARP-2 ($P < 0.01$), thereby excluding a major contribution of PARP-2 activation to the cellular response to H_2O_2 treatment.

Two compounds, namely BYK204165 and DPQ, exhibited low potency of PARP inhibition in C4I cells (pIC_{50} 5.75 and 5.47, respectively), which was apparently not compatible with inhibition of PARP-1 (pIC_{50} 7.35 and 6.43, respectively), but rather of PARP-2 (pIC_{50} 5.38 and 5.76, respectively) (Table 1). To address the possibility of PARP-2 rather than PARP-1

being involved in this cell type, we compared pIC_{50} values at mouse PARP-2 and human PARP-1 with those in C4I cells from eight compounds, *i.e.* BYK49187, BYK20370, BYK204165, PND, DPQ, 4-HQN, 3-AB and NA, capable of discriminating between both enzyme isoforms at least by a factor of 3. However, the correlations obtained under these conditions did not fit better with either PARP-2 ($r^2 = 0.92$, $P < 0.01$; slope = 0.87 ± 0.08, mean ± S.E.M., n = 8) or PARP-1 *($r^2 = 0.94$, $P < 0.01$; slope = 0.81 ± 0.10, mean ± S.E.M., n = 8) (not shown). Thus, this approach did not reveal any preference for PARP-2 over PARP-1 activation in response to H_2O_2 stimulation in human cervical carcinoma C4I cells, either.

In the rat model of regional myocardial ischemia and reperfusion used here, only treatment with BYK49187 at an intravenous dose of 3 mg/kg bolus plus infusion of the same dose for 2 h caused a significant reduction of infarct size of 22%, whereas BYK49187 (at 1 mg/kg), BYK236864 or BYK20370 (both at 1 or 3 mg/kg) were not effective. This finding is consistent with our data from ex vivo experiments, where blood samples taken after BYK49187 at 3 mg/kg i.v. produced a significant PARP-1 inhibition of 80%, revealing that the blood levels of this compound in the rat were obviously high enough to afford cardioprotection, whereas blood samples after 3 mg/kg BYK20370 failed to have a significant effect in this respect. The ability of BYK236864 blood samples to significantly inhibit PARP-1 ex vivo by more than 50%, but its unexpected failure to act cardioprotective could be due to the model, in which a 25 min ischemia might have been too severe, whereas a shorter ischemic period might have revealed a significant reduction of infarct size by the compound. It has also been argued that a much greater therapeutic benefit in conditions associated with the consequences of ischemia-reperfusion could be attained with more potent and water-soluble inhibitors of PARP. Available data from the literature, however, indicate no clear superiority of PARP inhibitors with good water-solubility (e.g. 3-AB, 5-AIQ, PJ34, INO-1001) over poorly water-soluble inhibitors (e.g. ISQ, GPI-6150), at least regarding reduction of infarct size in the rat heart. In line with our observation the maximally obtainable reduction of myocardial infarct size in the rat reported in the literature was 17 - 36% (Zingarelli et al., 1997; Pieper et al., 2000; Liaudet et al., 2001; Wayman et al., 2001; Faro et al., 2002). However, the cardiac infarct size in *parp-1*^{-/-} mice subjected to global myocardial ischemia and reperfusion is decreased by maximally 35% relative to untreated wild type mice, possibly due to a residual poly(ADP-ribosyl)ation activity mediated by alternative isoform(s) of PARP in this tissue (Pieper et al., 2000).

From the high degree of homology of the PARP catalytic domain between species, it has been suggested that PARP inhibitors might exhibit no difference in terms of potency in

human, rat and mouse tissues (de Murcia et al., 1994; Iwashita et al., 2004b; Iwashita et al., 2004c; Kinoshita et al., 2004), and it was speculated that none of the PARP inhibitors existing at that time would be able to discriminate between PARP-1 and PARP-2 (Oliver et al., 2004). However, Perkins and colleagues discovered compounds of the quinazolinone and phthalazinone structure with modest selectivity for PARP-1 and PARP-2, respectively (Perkins et al., 2001). Recently, distinct binding modes necessary for discrimination between ligands and each isoenzymes have been identified, enabling the synthesis of quinazolinones, e.g. FR247304, with selectivity for PARP-1, and quinoxalines, e.g. FR261529, with selectivity for PARP-2 (Iwashita et al., 2004a; Iwashita et al., 2004b; Ishida et al., 2006), thus demonstrating the feasibility of designing PARP-isoform selective ligands.

In terms of selectivity for PARP-1, BYK204165 outperforms that of recently reported quinazolinones, like FR247304, with 10- to 39-fold selectivity for PARP-1 over PARP-2 (Iwashita et al., 2004b; Ishida et al., 2006). The enzymatic selectivity of BYK204165 for PARP-1 over PARP-2 is maintained at the cellular level in *parp-1$^{+/+}$* and *parp-1$^{-/-}$* mouse fibroblasts. Our data clearly confirm the high selectivity of BYK204165 for inhibition of PARP-1, based on its failure to inhibit PARP-2 in both cell lines, whereas the unselective inhibitor BYK236864 completely abrogates PAR formation by both PARP-1 and PARP-2. The method employed here might provide a novel and convenient functional approach towards assessment of the contribution of PARP-1 and PARP-2 to DNA damage-induced PAR formation in intact cells, as the enzymatic activity of the two isoforms can be assessed by use of a selective PARP-1 inhibitor.

In conclusion, among the new compounds studied, the imidazoquinolinone BYK49187 emerged as a potent and reversible, but unselective PARP-1/2 inhibitor in various in vitro assays. This compound also reduced myocardial infarct size in the rat, whereas the less potent PARP inhibitors BYK236864 and BYK20370 did not. Furthermore, the isoquinolindione BYK204165 displayed 100-fold selectivity for PARP-1 and therefore may have two important uses, *i.e.* (i) as a lead for further drug development and (ii) as a tool to dissect cellular functions of PARP-1 and PARP-2. Thus, BYK49187, due to its high potency, and BYK204165, due to its high selectivity, represent novel and valuable tools for investigating PARP-1 mediated effects.

Acknowledgements

We thank Gilbert de Murcia (Illkirch-Graffenstaden, France) for *parp-1*$^{+/+}$ and *parp-1*$^{-/-}$

mouse embryonic fibroblasts. We gratefully acknowledge I. Gruhler, K. Graf, E. Herrmann

and S. Haas for excellent technical assistance.

References

Amè JC, Spenlehauer C and de Murcia G (2004) The PARP superfamily. Bioessays **26**:882-893.

Banasik M, Stedeford T, Strosznajder RP, Persad AS, Tanaka S and Ueda K (2004) The effects of organic solvents on poly(ADP-ribose) polymerase-1 activity: implications for neurotoxicity. Acta Neurobiol Exp (Wars) **64**:467-473.

Beneke S, Diefenbach J and Bürkle A (2004) Poly(ADP-ribosyl)ation inhibitors: promising drug candidates for a wide variety of pathophysiologic conditions. Int J Cancer **111**:813-818.

Bowes J, Ruetten H, Martorana PA, Stockhausen H and Thiemermann C (1998) Reduction of myocardial reperfusion injury by an inhibitor of poly (ADP-ribose) synthetase in the pig. Eur J Pharmacol **359**:143-150.

Calabrese CR, Almassy R, Barton S, Batey MA, Calvert AH, Canan-Koch S, Durkacz BW, Hostomsky Z, Kumpf RA, Kyle S, Li J, Maegley K, Newell DR, Notarianni E, Stratford IJ, Skalitzky D, Thomas HD, Wang LZ, Webber SE, Williams KJ and Curtin NJ (2004) Anticancer chemosensitization and radiosensitization by the novel poly(ADP-ribose) polymerase-1 inhibitor AG14361. J Natl Cancer Inst **96**:56-67.

Cheng Y and Prusoff WH (1973) Relationship between the inhibition constant (K_1) and the concentration of inhibitor which causes 50 per cent inhibition (I_{50}) of an enzymatic reaction. Biochem Pharmacol **22**:3099-3108.

D'Amours D, Desnoyers S, D'Silva I and Poirier GG (1999) Poly(ADP-ribosyl)ation reactions in the regulation of nuclear functions. Biochem J **342 (Pt 2)**:249-268.

de la Lastra CA, Villegas I and Sánchez-Fidalgo S (2007) Poly(ADP-ribose) polymerase inhibitors: new pharmacological functions and potential clinical implications. Curr Pharm Des **13**:933-962.

de Murcia G, Schreiber V, Molinete M, Saulier B, Poch O, Masson M, Niedergang C and Menissier de Murcia J (1994) Structure and function of poly(ADP-ribose) polymerase. Mol Cell Biochem **138**:15-24.

Docherty JC, Kuzio B, Silvester JA, Bowes J and Thiemermann C (1999) An inhibitor of poly(ADP-ribose) synthetase activity reduces contractile dysfunction and preserves high energy phosphate levels during reperfusion of the ischaemic rat heart. Br J Pharmacol **127**:1518-1524.

Eliasson MJ, Sampei K, Mandir AS, Hurn PD, Traystman RJ, Bao J, Pieper A, Wang ZQ, Dawson TM, Snyder SH and Dawson VL (1997) Poly(ADP-ribose) polymerase gene disruption renders mice resistant to cerebral ischemia. Nat Med **3**:1089-1095.

Faro R, Toyoda Y, McCully JD, Jagtap P, Szabo E, Virag L, Bianchi C, Levitsky S, Szabo C and Sellke FW (2002) Myocardial protection by PJ34, a novel potent poly (ADP-ribose) synthetase inhibitor. Ann Thorac Surg **73**:575-581.

Ishida J, Yamamoto H, Kido Y, Kamijo K, Murano K, Miyake H, Ohkubo M, Kinoshita T, Warizaya M, Iwashita A, Mihara K, Matsuoka N and Hattori K (2006) Discovery of potent and selective PARP-1 and PARP-2 inhibitors: SBDD analysis via a combination of X-ray structural study and homology modeling. Bioorg Med Chem **14**:1378-1390.

Iwashita A, Mihara K, Yamazaki S, Matsuura S, Ishida J, Yamamoto H, Hattori K, Matsuoka N and Mutoh S (2004a) A new poly(ADP-ribose) polymerase inhibitor, FR261529 [2-(4-chlorophenyl)-5-quinoxalinecarboxamide], ameliorates methamphetamine-induced dopaminergic neurotoxicity in mice. J Pharmacol Exp Ther **310**:1114-1124.

Iwashita A, Tojo N, Matsuura S, Yamazaki S, Kamijo K, Ishida J, Yamamoto H, Hattori K, Matsuoka N and Mutoh S (2004b) A novel and potent poly(ADP-ribose) polymerase-1 inhibitor, FR247304 (5-chloro-2-[3-(4-phenyl-3,6-dihydro-1(2H)-pyridinyl)propyl]-4(3H)-quinazo linone), attenuates neuronal damage in in vitro and in vivo models of cerebral ischemia. J Pharmacol Exp Ther **310**:425-436.

Iwashita A, Yamazaki S, Mihara K, Hattori K, Yamamoto H, Ishida J, Matsuoka N and
    Mutoh S (2004c) Neuroprotective effects of a novel poly(ADP-ribose) polymerase-1
    inhibitor, 2-[3-[4-(4-chlorophenyl)-1-piperazinyl] propyl]-4(3H)-quinazolinone
    (FR255595), in an in vitro model of cell death and in mouse 1-methyl-4-phenyl-
    1,2,3,6-tetrahydropyridine model of Parkinson's disease. J Pharmacol Exp Ther
    309:1067-1078.

Jagtap P and Szabó C (2005) Poly(ADP-ribose) polymerase and the therapeutic effects of
    its inhibitors. Nat Rev Drug Discov **4**:421-440.

Kinoshita T, Nakanishi I, Warizaya M, Iwashita A, Kido Y, Hattori K and Fujii T (2004)
    Inhibitor-induced structural change of the active site of human poly(ADP-ribose)
    polymerase. FEBS Lett **556**:43-46.

Liaudet L, Szabó E, Timashpolsky L, Virag L, Cziráki A and Szabó C (2001) Suppression
    of poly (ADP-ribose) polymerase activation by 3-aminobenzamide in a rat model of
    myocardial infarction: long-term morphological and functional consequences. Br J
    Pharmacol **133**:1424-1430.

McCabe N, Lord CJ, Tutt AN, Martin NM, Smith GC and Ashworth A (2005) BRCA2-
    deficient CAPAN-1 cells are extremely sensitive to the inhibition of Poly (ADP-
    Ribose) polymerase: an issue of potency. Cancer Biol Ther **4**:934-936.

McDonald MC, Mota-Filipe H, Wright JA, Abdelrahman M, Threadgill MD, Thompson AS
    and Thiemermann C (2000) Effects of 5-aminoisoquinolinone, a water-soluble,
    potent inhibitor of the activity of poly (ADP-ribose) polymerase on the organ injury
    and dysfunction caused by haemorrhagic shock. Br J Pharmacol **130**:843-850.

Oliver AW, Ame JC, Roe SM, Good V, de Murcia G and Pearl LH (2004) Crystal structure
    of the catalytic fragment of murine poly(ADP-ribose) polymerase-2. Nucleic Acids
    Res **32**:456-464.

Perkins E, Sun D, Nguyen A, Tulac S, Francesco M, Tavana H, Nguyen H, Tugendreich S,
    Barthmaier P, Couto J, Yeh E, Thode S, Jarnagin K, Jain A, Morgans D and
    Melese T (2001) Novel inhibitors of poly(ADP-ribose) polymerase/PARP1 and
    PARP2 identified using a cell-based screen in yeast. Cancer Res **61**:4175-4183.

Pieper AA, Verma A, Zhang J and Snyder SH (1999) Poly (ADP-ribose) polymerase, nitric
    oxide and cell death. Trends Pharmacol Sci **20**:171-181.

Pieper AA, Walles T, Wei G, Clements EE, Verma A, Snyder SH and Zweier JL (2000)
    Myocardial postischemic injury is reduced by poly(ADP-ribose) polymerase-1 gene
    disruption. Mol Med **6**:271-282.

Schlicker A, Peschke P, Bürkle A, Hahn EW and Kim JH (1999) 4-Amino-1,8-
    naphthalimide: a novel inhibitor of poly(ADP-ribose) polymerase and radiation
    sensitizer. Int J Radiat Biol **75**:91-100.

Schreiber V, Dantzer F, Amé J and de Murcia G (2006) Poly(ADP-ribose): novel functions
    for an old molecule. Nat Rev Mol Cell Biol **7**:517-528.

Shieh WM, Ame JC, Wilson MV, Wang ZQ, Koh DW, Jacobson MK and Jacobson EL
    (1998) Poly(ADP-ribose) polymerase null mouse cells synthesize ADP-ribose
    polymers. J Biol Chem **273**:30069-30072.

Southan GJ and Szabó C (2003) Poly(ADP-ribose) polymerase inhibitors. Curr Med Chem
    10:321-340.

Szabó G, Liaudet L, Hagl S and Szabó C (2004) Poly(ADP-ribose) polymerase activation
    in the reperfused myocardium. Cardiovasc Res **61**:471-480.

Thiemermann C, Bowes J, Myint FP and Vane JR (1997) Inhibition of the activity of
    poly(ADP-ribose) synthetase reduces ischemia-reperfusion injury in the heart and
    skeletal muscle. Proc Natl Acad Sci U S A **94**:679-683.

Virág L and Szabó C (2002) The therapeutic potential of poly(ADP-ribose) polymerase
    inhibitors. Pharmacol Rev **54**:375-429.

Wagner S, Hussain M, Beckert S, Ghani Q, Weinreich J, Hunt T, Becker H and
    Königsrainer A (2007) Lactate down-regulates cellular poly(ADP-ribose) formation
    in cultured human skin fibroblasts. Eur J Clin Invest **37**:134-139.

Wayman N, McDonald MC, Thompson AS, Threadgill MD and Thiemermann C (2001) 5-aminoisoquinolinone, a potent inhibitor of poly (adenosine 5'-diphosphate ribose) polymerase, reduces myocardial infarct size. Eur J Pharmacol **430**:93-100.

Woon EC and Threadgill MD (2005) Poly(ADP-ribose) polymerase inhibition - where now? Curr Med Chem **12**:2373-2392.

Yu SW, Wang H, Poitras MF, Coombs C, Bowers WJ, Federoff HJ, Poirier GG, Dawson TM and Dawson VL (2002) Mediation of poly(ADP-ribose) polymerase-1-dependent cell death by apoptosis-inducing factor. Science **297**:259-263.

Zhang J, Lautar S, Huang S, Ramsey C, Cheung A and Li JH (2000) GPI 6150 prevents H(2)O(2) cytotoxicity by inhibiting poly(ADP-ribose) polymerase. Biochem Biophys Res Commun **278**:590-598.

Zingarelli B, Cuzzocrea S, Zsengellér Z, Salzman AL and Szabó C (1997) Protection against myocardial ischemia and reperfusion injury by 3-aminobenzamide, an inhibitor of poly (ADP-ribose) synthetase. Cardiovasc Res **36**:205-215.

Legends to Figures

Fig. 1. Chemical structures of the imidazoquinolinones BYK49187 and BYK236864, the imidazopyridine BYK20370 and the isoquinolindione BYK204165.

Fig. 2. (**A**) Substrate dependency of human PARP-1 activity in the presence of increasing BYK49187 concentrations (10, 30, 100 and 300 nM). (**B**) Lineweaver-Burk plot, showing respective data from saturation experiments and revealing the competitive type of inhibition. (**C**) pK_i value for BYK49187 determined by Schild plot analysis (pK_i 7.97; intercept with the abscissa at a slope of 0.64). Each point represents the mean of duplicate determinations.

Fig. 3. (**A**) Substrate dependency of human PARP-1 activity in the presence of increasing BYK236864 concentrations (50, 125 and 400 nM). (**B**) Lineweaver-Burk plot, showing respective data from saturation experiments and revealing the competitive type of inhibition. (**C**) pK_i value for BYK236864 determined by Schild plot analysis (pK_i 7.43; intercept with the abscissa at a slope of 1.06). Each point represents the mean of duplicate determinations.

Fig. 4. (**A**) Substrate dependency of human PARP-1 activity in the presence of increasing BYK20370 concentrations (1, 3, 10 and 30 µM). (**B**) Lineweaver-Burk plot, showing respective data from saturation experiments and revealing the competitive type of inhibition. (**C**) pK_i value for BYK20370 determined by Schild plot analysis (pK_i 5.90; intercept with the abscissa at a slope of 0.94). Each point represents the mean of duplicate determinations.

Fig. 5. (**A**) Substrate dependency of human PARP-1 activity in the presence of increasing BYK204165 concentrations (30, 100, 300 nM, 1 and 3 µM). (**B**) Lineweaver-Burk plot, showing respective data from saturation experiments and revealing the competitive type of inhibition. (**C**) pK_i value for BYK204165 determined by Schild plot analysis (pK_i 7.05; intercept with the abscissa at a slope of 0.98). Each point is the mean of duplicate determinations.

Fig. 6. Immunofluorescence analysis of H_2O_2 induced PAR formation in cultured fibroblasts from *parp-1$^{+/+}$* (**A**) and *parp-1$^{-/-}$* (**B**) mice. No specific PAR staining is observed in the absence of H_2O_2 (-H_2O_2). H_2O_2 (+H_2O_2) induced PAR formation in *parp-1$^{+/+}$* fibroblasts (**A**) due to activation of both PARP-1 and PARP-2 is characterised by large

number of intense, granular signals in the cell nuclei and is totally inhibited by BYK236864 (0.3 – 10 µM), whereas residual PAR formation is detectable in the presence of BYK204165 (0.3 – 10 µM). Note that the "soft" staining visible in the panel +H_2O_2 +10 µM BYK236864 is non-specific cytoplasmic background (see below). In *parp-1$^{-/-}$* fibroblasts (**B**) H_2O_2 (+H_2O_2) induced PAR formation (arrows) due to activation of PARP-2 only is much weaker than in *parp-1$^{+/+}$* fibroblasts, as expected, and is abrogated in the presence of BYK236864 (0.3 – 3 µM) but remains unaffected by BYK204165 (0.3 – 3 µM). Note that the photographic exposure time for the *parp-1$^{-/-}$* samples was much longer, in view of the reduced overall signal intensity. As consequence, a non-specific, "soft", cytoplasmic background emerges in all *parp-1$^{-/-}$* samples, which is, however, easily distinguishable from the genuine, granular, intranuclear PAR signals.

Fig. 7. Concentration-response curves for inhibition of H_2O_2-activated PARP in human lung epithelial A549 cells (**A**) and in rat cardiac myoblast H9c2 cells (**B**) by BYK49187, BYK236864, BYK20370 and BYK204165. Given are means ± S.E.M. of 4 - 6 experiments.

Fig. 8. Correlation of pIC$_{50}$ values for BYK compounds and reference compounds to inhibit PARP in human lung epithelial A549 versus human cervical carcinoma C4I cells (**A**) (r^2 = 0.95, *P* < 0.001; slope = 0.97 ± 0.07, mean ± S.E.M., n = 12), and versus rat cardiac myoblast H9c2 cells (**B**) (r^2 = 0.97, *P* < 0.001; slope = 1.05 ± 0.06, mean ± S.E.M., n = 13). The numbering of the reference compounds refers to their listing in Table 1.

Fig. 9. (**A**) Correlation of pIC$_{50}$ values for BYK compounds and reference compounds to inhibit cell-free human PARP-1 versus human lung epithelial A549 cells (top; r^2 = 0.89, *P* < 0.001; slope = 0.78 ± 0.08, mean ± S.E.M., n = 13), versus human cervical carcinoma C4I cells (middle; r^2 = 0.92, *P* < 0.001; slope = 0.83 ± 0.08, mean ± S.E.M., n = 12), and versus rat cardiac myoblast H9c2 cells (bottom; r^2 = 0.96, *P* < 0.001; slope = 0.87 ± 0.06, mean ± S.E.M., n = 13). (**B**) Correlation of pIC$_{50}$ values for BYK compounds and reference compounds to inhibit cell-free murine PARP-2 versus human lung epithelial A549 cells (top; r^2 = 0.78, *P* < 0.01; slope = 0.71 ± 0.11, mean ± S.E.M., n = 13), versus human cervical carcinoma C4I cells (middle; r^2 = 0.84, *P* < 0.01; slope = 0.79 ± 0.11, mean ± S.E.M., n = 12), and versus rat cardiac myoblast H9c2 cells (bottom; r^2 = 0.83, *P* < 0.01; slope = 0.79 ± 0.11, mean ± S.E.M., n = 13).

Fig. 10. (**A**) Area at risk (AAR) and (**B**) infarct size after regional myocardial ischemia (25 min) and reperfusion (2 h) in the anesthetised rat treated with BYK49187. The animals were subjected to the surgical procedure alone (Sham, n = 10) or subjected to coronary

artery occlusion and reperfusion and treated with either vehicle (n = 11) or with BYK49187 at 1 mg/kg i.v. bolus followed by 1 mg/kg/h i.v., or 3 mg/kg i.v. bolus followed by 3 mg/kg/h i.v. (each n = 10). Given are means ± S.E.M. * $P < 0.05$ when compared to vehicle. (**C**) Blood samples drawn at the end of infusion (2 h) of the test drugs BYK20370, BYK236864 and BYK49187 (each at 3 mg/kg i.v.) were analysed ex vivo for their ability to inhibit human PARP-1 (in the presence of DNA). Resulting enzyme activities expressed as cpm per sample are depicted as data points of 7-15 samples for each treatment with mean values thereof. *** $P < 0.001$ compared to sham. n.s., not significant.

TABLE 1

Potencies of BYK49187, BYK236864, BYK20370 and BYK204165 in comparison with reference compounds to inhibit cell-free human PARP-1, mouse PARP-2 and H_2O_2-activated cellular PARP in human lung epithelial A549, human cervical carcinoma C4I and rat cardiac myoblast H9c2 cells. Inhibitory potencies are expressed as pIC_{50} values with slope values (in parentheses) of the concentration-response curves. Given are means ± S.E.M. of n = 3 - 5 experiments for hPARP-1 and mPARP-2, and n = 4 - 6 experiments for each cellular PARP assay and compound.

Compound	hPARP-1	mPARP-2	A549 cells	C4I cells	H9c2 cells	logP
BYK49187	8.36 ± 0.11 (1.08)	7.70 ± 0.13 (0.93)	7.80 ± 0.08	7.02 ± 0.11	7.65 ± 0.03	2.3
BYK236864	7.81 ± 0.09 (1.13)	7.55 ± 0.10 (0.89)	6.41 ± 0.03	n.t.	6.70 ± 0.03	3.8
BYK20370	6.40 ± 0.13 (1.17)	5.71 ± 0.14 (1.05)	6.51 ± 0.14	6.05 ± 0.09	6.02 ± 0.04	2.5
BYK204165	7.35 ± 0.10 (0.96)	5.38 ± 0.08 (1.08)	6.64 ± 0.15	5.75 ± 0.07	6.91 ± 0.05	2.3
PJ34 [1]	7.72 ± 0.08 (0.93)	7.21 ± 0.06 (1.19)	n.t.	n.t.	n.t.	1.6
4-ANI [2]	7.66 ± 0.09 (1.24)	7.49 ± 0.05 (1.03)	6.88 ± 0.06	6.24 ± 0.12	6.94 ± 0.08	1.4
GPI-6150 [3]	7.08 ± 0.14 (1.31)	6.73 ± 0.17 (1.03)	6.81 ± 0.11	6.25 ± 0.11	6.86 ± 0.12	2.6
PND [4]	7.07 ± 0.13 (1.39)	6.48 ± 0.16 (0.91)	6.77 ± 0.13	6.37 ± 0.15	6.62 ± 0.12	2.2
ISQ [5]	6.82 ± 0.11 (1.09)	6.35 ± 0.13 (0.87)	6.51 ± 0.09	5.47 ± 0.09	6.51 ± 0.11	2.4
DPQ [6]	6.43 ± 0.14 (1.07)	5.76 ± 0.13 (0.75)	6.60 ± 0.17	5.47 ± 0.12	6.64 ± 0.03	2.5
5-AIQ [7]	5.93 ± 0.07 (1.02)	5.74 ± 0.08 (1.18)	n.t.	n.t.	n.t.	-0.4
4-HQN [8]	5.23 ± 0.11 (1.16)	4.59 ± 0.09 (1.01)	4.97 ± 0.12	4.46 ± 0.11	4.84 ± 0.10	1.7
INH$_2$BP [9]	5.07 ± 0.17 (0.95)	4.75 ± 0.11 (0.98)	4.80 ± 0.08	3.87 ± 0.09	4.62 ± 0.04	1.9
3-AB [10]	4.89 ± 0.09 (1.06)	4.38 ± 0.06 (1.01)	4.95 ± 0.11	4.16 ± 0.11	4.81 ± 0.14	-0.3
NA [11]	4.30 ± 0.08 (1.13)	3.68 ± 0.10 (1.25)	4.29 ± 0.12	3.73 ± 0.17	4.10 ± 0.11	-0.2

Numbering of the reference compounds [in brackets] refers to Fig. 8. Abbreviations: BYK49187, 2-[4-(5-methyl-1*H*-imidazol-4-yl))-piperidin-1-yl]-4,5-dihydro-imidazo[4,5,1-i,j]quinolin-6-one. BYK236864, 2-(4-pyridin-2-yl-phenyl)-4,5-dihydro-imidazo[4,5,1-i,j]quinolin-6-one. BYK20370, 6-chloro-8-hydroxy-2,3-dimethyl-imidazo-[1,2-α]-pyridine. BYK204165, 4-(1-methyl-1*H*-pyrrol-2-ylmethylene)-4*H*-isoquinoline-1,3-dione. DPQ, 3,4-dihydroxy-5-[4-(piperidin1-yl)butoxy]isoquinolin-1(2*H*)-one. PND, 6-(5*H*)-phenanthridinone. ISQ, 1,5-dihydroxyisoquinoline. NA, nicotinamide. 3-AB, 3-aminobenzamide. 5-AIQ, 5-aminoisoquinolin-1(2*H*)-one. PJ34, N-(6-oxo-5,6-dihydro-phenanthridin-2-yl)-N,N-dimethylacetamide. GPI-6150, 1,11b-dihydro-[2*H*]benzo-pyrano[4,3,2-de]isoquinolin-3-one. 4-ANI, 4-amino-1,8-naphthalimide. 4-HQN, 4-hydroxyquinazoline. INH$_2$BP, 5-iodo-6-amino-1,2-benzopyrone. n.t. not tested. LogP values were calculated by Hansch method.
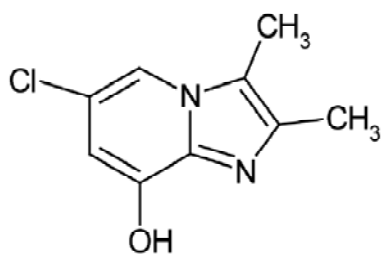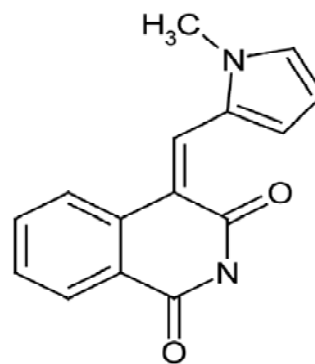
Fig. 1
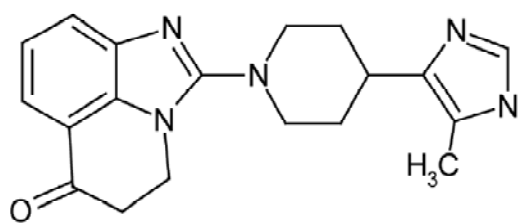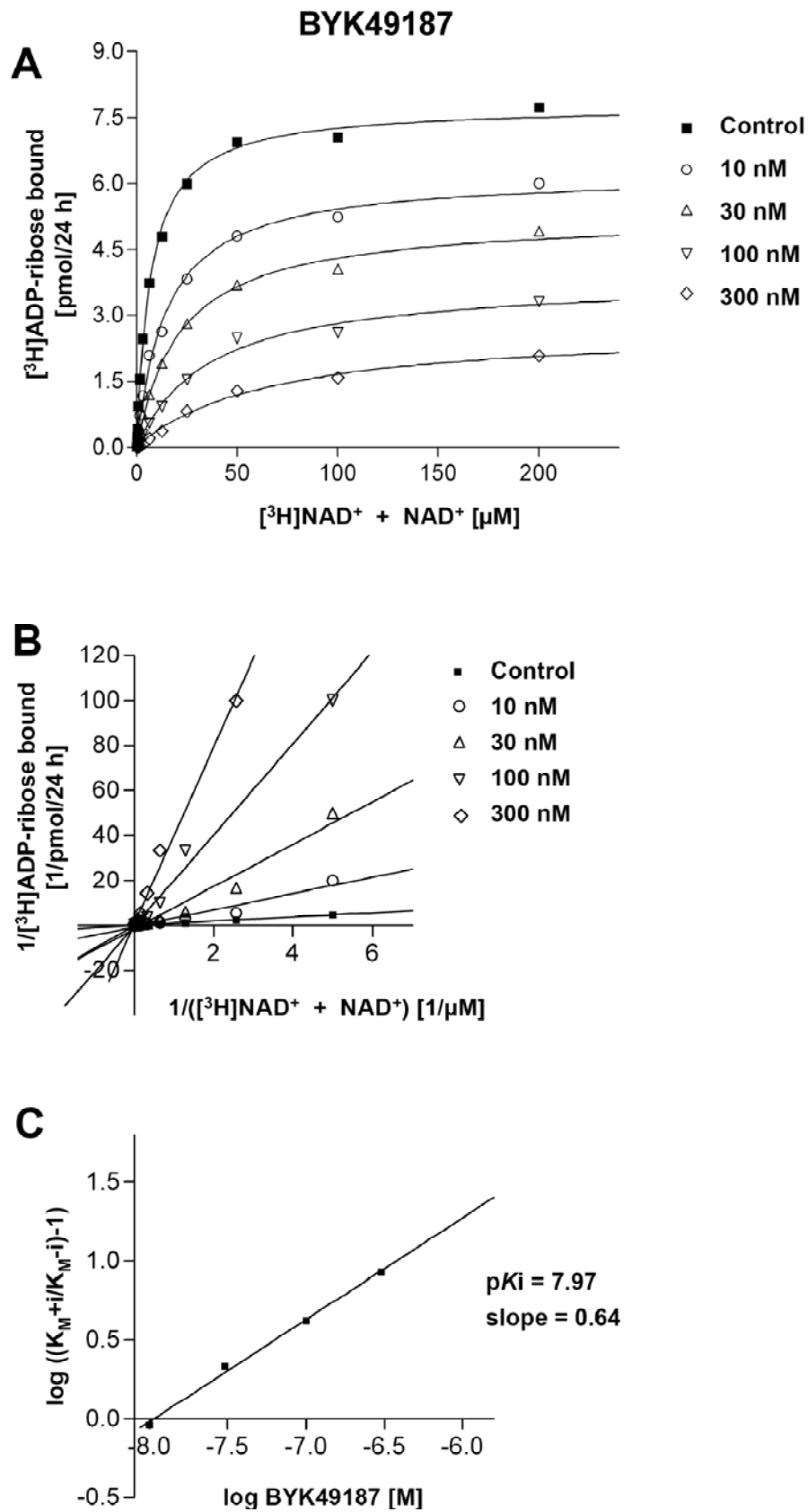

BYK49187
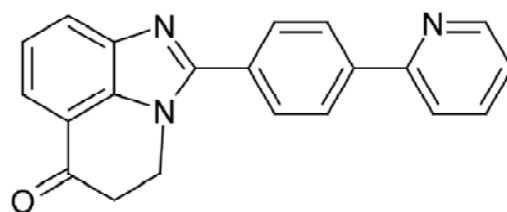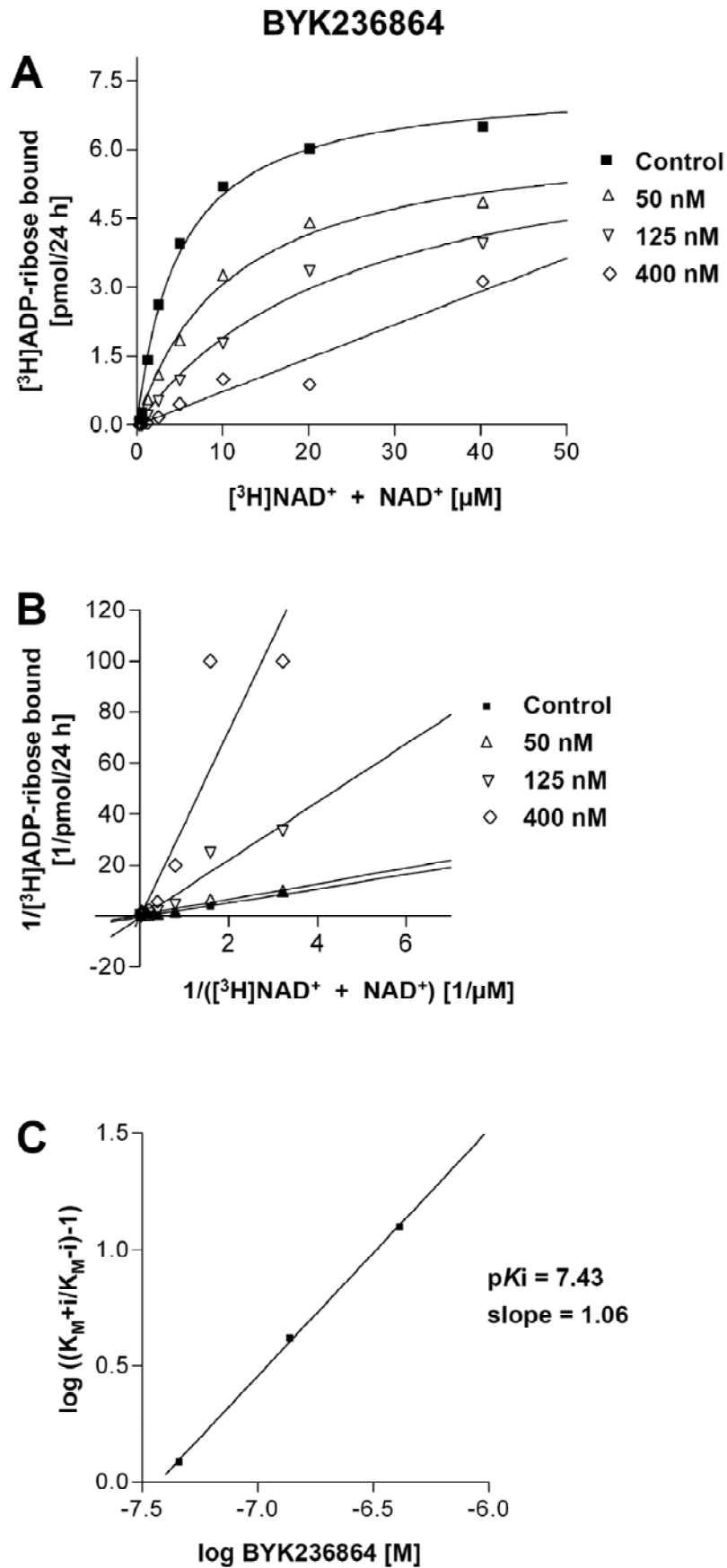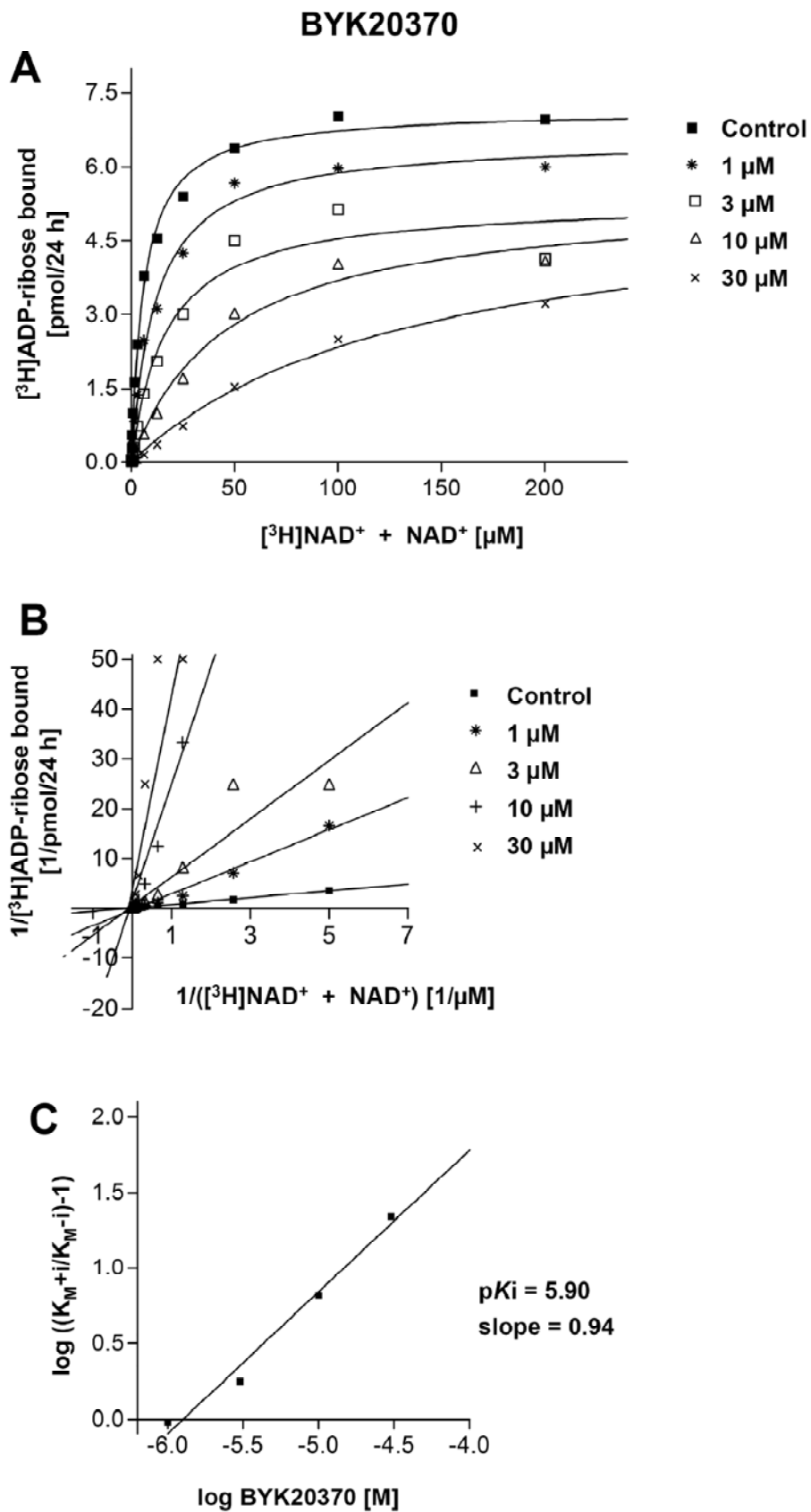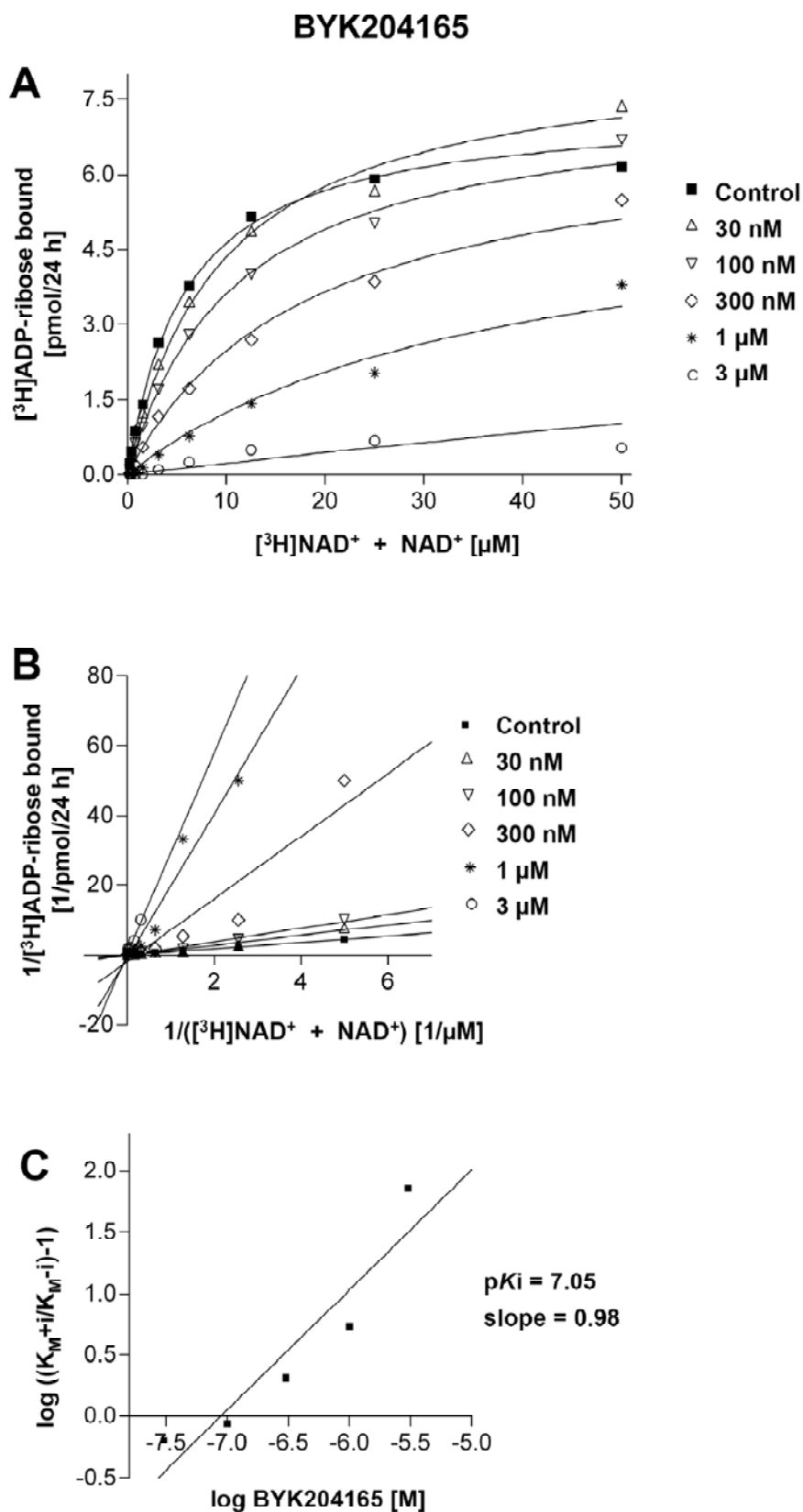
BYK236864

BYK20370
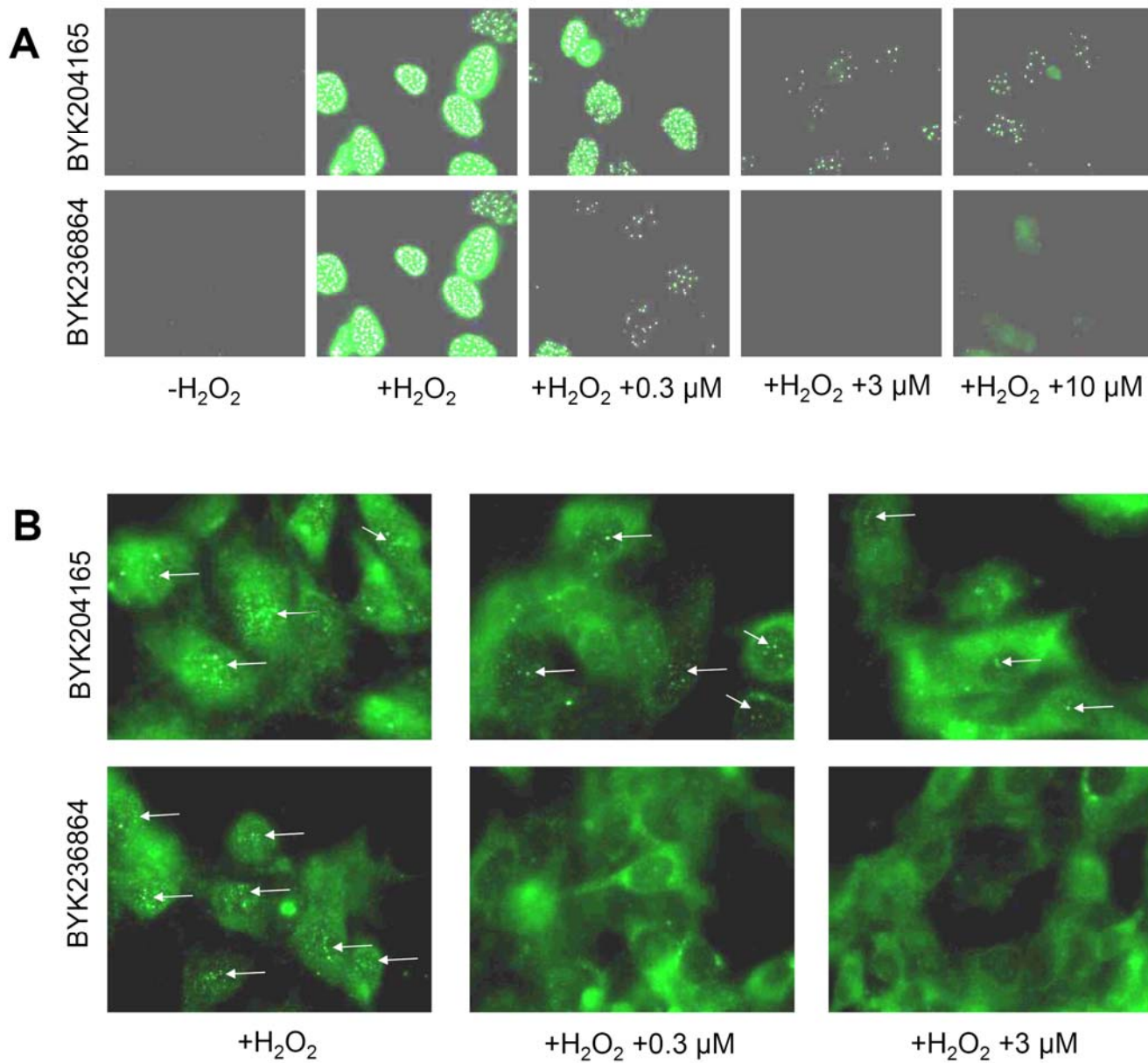
BYK204165

Fig. 2

Fig. 3

Fig. 4

Fig. 5

Fig. 6

Fig. 7

A549 cells

H9c2 cells

Fig. 8

Fig. 9

Fig. 10